Interim Report for Phase II – Task 1 of the Comprehensive Study to Understand Longitudinal ERW Seam Failures

"Hydrostatic Testing Protocols"

Authors

Bruce A. Young and Richard J. Olson

Battelle Memorial Institute
505 King Avenue
Columbus, OH 43201

Prepared for

U.S. Department of Transportation
Pipeline and Hazardous Materials Safety Administration
1200 New Jersey Ave., SE
Washington DC 20590

Contract No. DTPH56-11-T-000003
Battelle Contract No. G006084
Battelle Project No. 100004552

May 2017

Battelle does not engage in research for advertising, sales promotion, or endorsement of our clients' interests including raising investment capital or recommending investments decisions, or other publicity purposes, or for any use in litigation.

Battelle endeavors at all times to produce work of the highest quality, consistent with our contract commitments. However, because of the research and/or experimental nature of this work the client undertakes the sole responsibility for the consequence of any use or misuse of, or inability to use, any information, apparatus, process or result obtained from Battelle, and Battelle, its employees, officers, or Directors have no legal liability for the accuracy, adequacy, or efficacy thereof.

© 2017 Battelle
This publication may not be reproduced or distributed without the prior written permission of the copyright owner.

Acknowledgments

Useful discussions during this phase of the project with B.N. Leis of B.N. Leis, Inc. are acknowledged.

Executive Summary

On November 1, 2007 a liquid propane pipeline operated by Dixie Pipeline Company ruptured near Carmichael, Mississippi, which several pipeline industry experts collaboratively indicated the origin was likely a defect in the longitudinal Electric Resistance Welded (ERW) seam, with the ensuing fracture running along that joint into portions of the adjacent pipes. These experts also noted that a seam-integrity assessment did not prevent the failure, as this failure came 2 years after an in-line inspection (ILI) with a sophisticated crack-detection tool; and 23 years after a hydrostatic test to a hoop stress level greater than 1.25 times the maximum operating hoop stress level. Following the National Transportation Safety Board's (NTSB) public report, the NTSB issued Recommendation P-09-1, which called upon the Department of Transportation Pipeline and Hazardous Material Safety Administration (DOT-PHMSA) to conduct a comprehensive study to identify actions that can be used by operators to eliminate catastrophic longitudinal seam failures in pipe, and indicated the required scope. This led to the PHMSA- issued research announcement (RA) that targeted Recommendation P-09-1 in the form of Broad Agency Announcement (BAA) Solicitation DTPH56-11-RA-000001. That Solicitation sought a Comprehensive Understanding of Longitudinal ERW Seam Failures.

In response to that Solicitation, Battelle, as the prime contractor, proposed a two-phase project to work to develop the understanding sought by the research announcement in resolving Recommendation P-09-1.

The Phase I final report was issued in January 2014 and can be found at the following website: https://primis.phmsa.dot.gov/matrix/PrjHome.rdm?prj=390. Phase II has five tasks including:

- Task 1: Hydrotest protocols
- Task 2: ILI and In-the-Ditch-Method (ITDM) Inspection Assessment
- Task 3: Defect Characterization: Types, Sizes, Shapes, and Idealizations

- Task 4: Model Validation
- Task 5L: Software Development for Integrity Management of Long Seam Welds.

This report focuses on the results obtained during the work completed under Phase II, Task 1 which includes the investigation of hydrostatic testing protocols. Details of the analysis methods used in the development of the results are provided along with a discussion the results and recommendations.

Contents

Acknowledgments iii

Executive Summary iii

Acronyms vii

Introduction 1

Overview 1

Study Parameters and Models 2

- Material Properties 3
- Pressure Characterization 4
- Time-Dependent Parameters 5
- Fatigue Models and Parameters 5

Results 7

- Area of Non-Analysis 8
- Cold Weld Analyses – X42 9
- Cold Weld Analyses – X80 15
- Hook Crack Analyses 17
- Selective Seam Weld Analyses 19

Conclusions and Discussion 21

Works Cited 23

List of Tables

Table 1: Design Space for Hydrotest Protocol for Cold Welds 3
Table 2: Static Material Properties as a Function of Pipe Grade 3
Table 3: Variable Values Used in Previous Studies 4
Table 4: Variable Values Used in This Report 4
Table 5: Parameters as a Function of Times for X42 and X80. 5
Table 6: Pressures Used during Fatigue Analyses 7
Table 7: Possible Scenarios for Hydrostatic Test Simulation 9
Table 8: Analyses Comparisons of Interest 10
Table 9: Summary Comparisons for X42 using a Cold-Weld Anomaly 14
Table 10: Analyzed Scenarios for Hydrostatic Test Simulation for Cold Weld X80 15
Table 11: Summary Comparisons for X80 using a Cold-Weld Anomaly 17

List of Figures

Figure 1: Invalid Analysis Region for X42 Cold-Weld Cracks at 72% SMYS 8
Figure 2: Simulated Hydrostatic Testing Results for X42 ID Cold-Weld using Scenario 1 10
Figure 3: Simulated Hydrostatic Testing Results for X42 ID Cold-Weld using Scenario 2 11
Figure 4: Simulated Hydrostatic Testing Results for X42 ID Cold-Weld using Scenario 3 11
Figure 5: Simulated Hydrostatic Testing Results for X42 ID Cold-Weld using Scenario 4 12
Figure 6: Simulated Hydrostatic Testing Results for X42 ID Cold-Weld using Scenario 5 12
Figure 7: Simulated Hydrostatic Testing Results for X42 ID Cold-Weld using Scenario 6 13
Figure 8: Simulated Results for X80 ID Cold-Weld using Scenario 1.....15
Figure 9: Simulated Results for X80 ID Cold-Weld using Scenario 2.....16
Figure 10: Simulated Results for X80 ID Cold-Weld using Scenario 3.....16
Figure 11: PipeAssess PI™ Hook Crack Geometry Idealization.....18

Acronyms

BAA	Broad Agency Announcement
CVN	Charpy V-Notch Toughness
DOT	Department of Transportation
ERW	Electric Resistance Welded
ID	Inner Diameter
ILI	Inline Inspection
ITDM	In the Ditch Method
MAOP	Maximum Allowable Operating Pressure
NTSB	National Transportation Safety Board
PHMSA	Pipeline and Hazardous Material Safety Administration
PipeAssess PI™	Battelle's Cracking Assessment for Pipeline software
R-ratio	Stress Ratio of minimum stress divided by maximum stress
RA	Research Announcement
SIF	Stress Intensity Factor
SMYS	Specified Minimum Yield Stress
a	Crack depth through the pipe wall
2C	Total crack length in the axial direction
t	Pipe Wall Thickness
D	Pipe Diameter
E	Young's Modulus
YS	Yield Strength
UTS	Ultimate Tensile Strength
σ	Stress
ε	Strain
α	Coefficient in the Ramberg-Osgood stress-strain representation
n	Exponent in the Ramberg-Osgood stress-strain representation
σ_0	Reference Stress
σ_F	Flow Stress (average yield stress and ultimate stress)
ε_0	Reference Strain (Reference Stress divided by Young's Modulus)
J_{IC}	Critical value of the elastic-plastic fracture toughness
dJ/da	Change in toughness with respect to the change in crack size
CVN	Charpy V-Notch value
K	Stress Intensity Factor
K_{max}	Maximum Stress Intensity Factor during a Fatigue Cycle
K_{min}	Minimum Stress Intensity Factor during a Fatigue Cycle
ΔK	Stress Intensity Factor Range (K_{max}- K_{min})
a/t	Normalized crack depth to the wall thickness
2C/a	Aspect Ratio of crack (length to depth)

Introduction

Work under Phase I followed a scope identified from National Transportation Safety Board (NTSB) Recommendation P-09-1 that developed understanding of longitudinal Electric Resistance Welded (ERW) seam failures by: 1) generating a database that quantified the industry and Government experience in regard to hydrotest and in-service failures, 2) completing a full-scale project that empirically quantified ERW seam failure behavior and resistance, and 3) developing technology to assess susceptibility to selective seam corrosion. Phase II builds on that understanding by establishing the viability of condition monitoring technology that relies on hydrotesting, in-line non-destructive inspection, and in-the-ditch nondestructive inspection along with the development of the engineering tools to translate condition into viable metrics of defect severity and re-inspection interval specific to ERW seam defects. Viability in all aspects will be assessed and demonstrated through use of full-scale burst tests that address the range of defects characteristics across that seen in the database developed in the initial phase of this of project. Management tools will be developed for use by pipeline operators as part of their integrity management plan to assure that their ERW pipelines are safe. This report focuses on the results obtained during the work completed under Phase II, Task 1 using the PipeAssess PI™ software developed under Phase II, Task 5.

Overview

This task analyzes various crack geometries under various loading conditions, including hydrostatic testing and fatigue, to investigate hydrostatic testing protocols. Based on the results of these analyses, compare and contrast scenarios were defined to elucidate the recommendations provided. Three major crack types were invested to ensure the recommended protocol met spirit of the competing outcomes. The crack type can be categorized as cold weld, hook, and selective seam weld corrosion cracks. The selection of hydrotest test pressure (spike and hold), along with the corresponding hold times, is neither obvious nor simple. The values that are considered the “best” must satisfy conflicting desired outcomes. On one hand, the desire is to remove all flaws which are near critical or which will become critical over some operational time (i.e.

operational pressure and fatigue). The counter desire is to limit the flaw growth during hydrotesting so that existing flaws will not become critical over the same operational time [1,2]. Numerous papers at the 2016 ASME IPC conference were focused on hydrostatic testing or pressure over-loads to retard crack growth. These papers are listed as reference [3-10].

The assumption for the overall strategy is that the pipeline operator has just inspected the pipe using ILI, ITDM, or both. Based on the knowledge of the flaws located in the line, the operator will then attempt a hydrostatic test, either as part of a general procedure or as part of the procedure for the replacement of a segment of pipe found to have a critical flaw. The overall objective of this assessment is to determine an optimized procedure which would expose near-critical flaws during the hydrotest, while minimizing the growth of pre-existing flaws. To determine hypothetical survivability between inspections and/or hydrotests (i.e. ensure pre-existing flaws do not become critical), hypothetic fatigue scenarios [11] over a period of five years was conducted after the simulated hydrostatic test. At the end of the fatigue scenario, a comparison of the failure pressure using the hypothetical crack size after flaw growth to the Maximum Allowable Operating Pressure (MAOP) (i.e. 72% of the Specified Minimum Yield Strength (SMYS)) was conducted. If the failure pressure was greater than MAOP, the crack was characterized as “survived”, otherwise, it was characterized as “failed after fatigue”. If the crack fails during the original hydrotest, the crack is characterized as “failed during hydrotest” [3].

Study Parameters and Models

To investigate strategies for developing an optimized hydrotest protocol, a parametric study was required. Table 1 provides an overview of the values used for the parametric study using a cold weld crack geometry such that X42 and X80 provide bounding material properties. Reference [3] provided the guidance required to develop a revised set of parameters. The total number of permutations for a full-factorial analysis was 3,072. The following sections outline the specifications (i.e. properties used) within the design space.

Table 1: Design Space for Hydrotest Protocol for Cold Welds

Variable	Values
Pipe Grades	X42, X80
Crack Depth (a/t)	0.05, 0.10, 0.15, 0.20, 0.35, 0.50, 0.65, 0.80
Crack Aspect Ratio (c/a)	2, 5, 10, 25
Pipe Size (D and t)	D=24.0" and t=0.281"
Charpy Values (ft-lbs)	1.0, 4.0, 15.0
Spike Pressure (% SMYS)	100, 110
Spike Time (min)	10, 30
Hold Pressure (% SMYS)	90
Hold Time (hours)	24

Material Properties

Time-dependent material properties for a range of pipe grades were obtained from References [1] and [2]. These pipe grades were used as the baseline for conducting the investigations into the hydrotest protocols. The static material properties for the materials used in this investigation span a range from Grade X42 to Grade X80. Table 1 provides the details of the static properties used.

Table 2: Static Material Properties as a Function of Pipe Grade

Grade	**X42**	**X80**
SMYS (ksi)	42.0	80
E (ksi)	29,000	29,000
YS (ksi)[1]	46.2	88.0
UTS (ksi)[2]	70.0	96.0
σ_0 (ksi)[3]	40.0	88.0
σ_F (ksi)[4]	58.1	92.0
ε_0 (in/in x 10^{-3})[5]	1.379	3.034
α[6]	1.019	0.130
n[6]	9.037	22.240

Note 1: Historical Reports indicate the typical YS is approximately 1.1xSMYS
Note 2: Historical Database Averages
Note 3: σ_0 is an arbitrary reference stress
Note 4: σ_F is the Average of the Yield and Ultimate
Note 5: ε_0 is the σ_0 /E
Note 6: Ramberg-Osgood properties from the time-dependent properties at time equal zero.

The following empirical correlations from Reference [2] were used to calculate the fracture parameters for the material resistance curve based on the Charpy values in Table 1.

$$J_{IC} = 0.1291 * \sigma_F * CVN \quad (1)$$

$$\frac{dJ}{da} = 1.082x10^5 * \frac{\sigma_F * CVN}{E} \quad (2)$$

Pressure Characterization

References [2] and [3] indicate that for gas lines, a set of optimum parameters were achieved using a pressure design space like that shown in Table 3. Because the flaw geometries between that study and this study are similar, the Reference [2] matrix has been revised as shown in Table 4. It should be noted that if an operator has a Maximum Allowable Operating Pressure (MAOP) of 72% SMYS and the hydrotest is completed at 1.25*MAOP; this scenario is equivalent to the operator conducting the hydrotest at 90% of SMYS. The use of 80% of SMYS in previous studies was for comparison purposes only, and should not be taken as a suggestion for testing at 80% SMYS; thus, the leak-check portion of 90% SMYS was used herein.

Table 3: Variable Values Used in Previous Studies [3]

Spike %SMYS	100, 110
Spike Hold Time (min)	30, 60
Hold %SMYS	80, 90
Hold Time (hrs)	24

Table 4: Variable Values Used in This Report

Spike %SMYS	100, 110
Spike Hold Time (min)	10, 30
Hold %SMYS	90
Hold Time (hrs)	24

Time-Dependent Parameters

The material response curve (i.e. stress-strain curve) is represented by the Ramberg-Osgood relationship provided in Equation (3) such that α and n are time-dependent under static, high-stress conditions such as conducting a hydrostatic test. [3]

$$\frac{\varepsilon}{\varepsilon_0} = \frac{\sigma}{\sigma_0} + \alpha(t)\left(\frac{\sigma}{\sigma_0}\right)^{n(t)} \tag{3}$$

This time-dependency can be determined via creep testing to obtain the instantaneous values of these parameters. Several tests were conducted as part of the NG-18 studies [1]. For these tests, specific values were obtained, along with a scheme to adjust these values with a given yield and ultimate within a particular Grade. Based on this information, Table 5 provides the details of the time-dependent parameters used for this study. As discussed in Reference [1], this time dependency effects the fracture mechanics resistance of the material during the applied deformation.

Table 5: Parameters as a Function of Times for X42 and X80.

Grades		X42			X80	
Time (sec)		α	n		α	n
0		1.019	9.037		0.130	22.240
0.1		1.662	9.027		0.145	22.240
1		2.693	9.018		0.161	22.250
10		4.334	9.009		0.179	22.260
60		6.246	9.001		0.195	22.270
120		7.188	8.998		0.201	22.270
300		8.646	8.995		0.210	22.270
600		9.935	8.992		0.216	22.270
3600		14.193	8.984		0.235	22.280
36000		22.317	8.976		0.262	22.290
360000		34.872	8.966		0.291	22.290

Fatigue Models and Parameters

The fatigue crack growth models used for this study have been chosen from various models currently used in industry. Based on vast amounts of testing, it has been shown that regardless of the specific crack geometry, if two cracks in the same material have the same stress intensity factor range ($\Delta K = K_{max} - K_{min}$) corresponding to the stress

intensity factor at maximum stress, σ_{max}, and minimum stress, σ_{min}, over a loading cycle), they will grow at the same rate and this growth rate will generically be represented by Equation (4). Below some value of ΔK, ΔK_{th}, the crack growth rate will be so small as to be undetectable. The growth behavior of most observable cracks is characterized by the Paris Equation, Equation (4), where the growth rate is linear on a log-log scale.

$$\frac{da}{dN} = C(\Delta K)^{\tilde{n}} \quad \Delta K > \Delta K_{th}$$
$$\frac{da}{dN} = 0 \quad \Delta K \leq \Delta K_{th} \tag{4}$$

The specific crack growth rate is also dependent on the loading ratio (σ_{min}/ σ_{max}). This can be accounted for in the Walker form of Equation (4) effect [13], and as shown in Equation (5).

$$\frac{da}{dN} = C\left(\frac{\Delta K}{\left(1-\frac{K_{min}}{K_{max}}\right)^{1-m}}\right)^{\tilde{n}} \quad \Delta K > \Delta K_{th}$$
$$\frac{da}{dN} = 0 \quad \Delta K \leq \Delta K_{th} \tag{5}$$

The fatigue model that is being employed for the software includes a crack retardation model which compensates for the reduction in crack growth due to plasticity induced crack closure as a function of applied stress. Most retardation models base the magnitude of the effect on the Irwin plastic zone size in front of the crack which is given by Equation (6).

$$r_p = \frac{1}{6\pi}\left(\frac{K_{max}}{YS}\right)^2 \tag{6}$$

The model used in PipeAssess PI™ is the Willenborg model [14]. Effectively, Willenborg's model says that when a higher stress occurs at a crack and then is subsequently relieved during unloading, a compressive stress field is generated in front of the crack tip. This compressive stress field reduces the effective stress on the crack tip so that the stress intensity factor is reduced. This is accomplished by substituting the maximum and minimum effective stresses for the actual stresses.

For the pipeline pressure cycle problem, crack retardation due to crack-tip plasticity is an ongoing phenomenon. Starting from a relatively higher pressure, crack growth will be retarded until the crack has grown sufficiently that the current plastic zone touches the plastic zone created during the overpressure. After that, new plastic zones will continue to be developed and overcome, depending on the loading.

In Reference [3], a set of proprietary fatigue cycles, modeled after a pipeline operator's pressure-time history [15], was converted to a generic monthly operating history, was developed. For this study, Reference [11] was used to develop two sets of fatigue parameters. Table 6 provides the fatigue histories used.

Table 6: Pressures Used during Fatigue Analyses

	%SMYS			Cycles per year	
Block	Max	Min	Delta	Very Aggressive	Light
1	72	0	72	20	0
2	72	7	65	40	0
3	72	17	55	100	0
4	72	27	45	500	25
5	72	37	35	1000	50
6	72	47	25	2000	100

Based on the information provided in Table 6, the cycles were applied in the following order: Year 1: Blocks 1 through 6; Year 2: Blocks 6 through 1; Repeat Year 1…etc. until reach the end of Year 5. It should be noted that the work completed in Reference [11] used a standard Paris-Law relationship with regard for R-ratio or stress intensity threshold. This type of model tends to be very conservative.

Results

Analyses were conducted on cold weld crack like features. Results are discussed in the context of the variation between hook cracks to cold weld cracks variation and the selective seam weld corrosion crack to cold weld cracks variation. Based on the input discussed in the previous sections, the results of these analyses are shown in the following sections of the report.

Area of Non-Analysis

As indicated in Table 6, the maximum value of the fatigue cycle is 72% SMYS. As indicated in the assumptions of this study, the MP or MAOP is also 72% SMYS. Based on this information, there is a set of crack sizes which will not tolerate 72% SMYS, and as such should not be analyzed or be indicated as invalid crack sizes because they would have failed in-service prior to the application of the hypothetic hydrostatic test. For example, those crack sizes shown in Figures 1 for the cold-weld crack analyses provide an indication of those points considered valid or invalid.

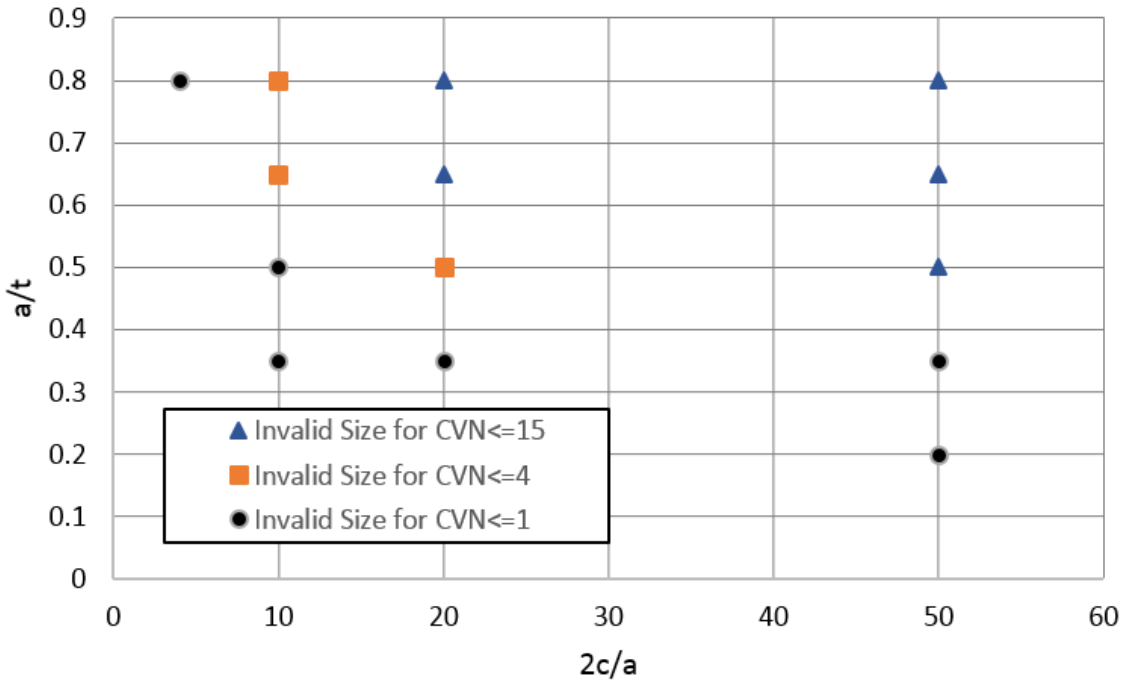

Figure 1: Invalid Analysis Region for X42 Cold-Weld Cracks at 72% SMYS (normalized crack depth to crack aspect ratio)

Thus, for certain analyses the upper right corner of the failure diagram will be invalid based on the anomaly feature. The specific region will be based on a combination of crack geometry and material toughness. For example, the invalid region for the hook-crack anomalies is smaller due to the driving force being reduced due to the analyzed flaw being an embedded flaw rather than a surface crack.

Cold Weld Analyses – X42

Analyses were completed to simulate several loading scenarios on various size cold-welds. These scenarios are outlined in Table 7. For all scenarios, the fatigue cycles were applied for 5 years and the leak-check pressure was 90% of the pressure at SMYS for the balance of 24 hours.

Table 7: Possible Scenarios for Hydrostatic Test Simulation (See Table 6)

Scenario	Spike Stress (%SMYS)	Spike Hold (min)	Fatigue
1	100	10	Very Aggressive
2	100	30	Very Aggressive
3	110	10	Very Aggressive
4	110	30	Very Aggressive
5	100	10	Light
6	100	30	Light
7	110	10	Light
8	110	30	Light
9	N/A	N/A	Very Aggressive
10	N/A	N/A	Light

While there are ten scenarios for each combination of material and crack geometry, Table 8 provides a useful matrix for determining the comparisons undertaken in this study. Figures 2 through 7, provide the results for the analyses in Table 7.

It should be noted that for the crack size of a/t=0.8, 2c/a=4, and a CVN of 4.0, the failure resulted during the simulated hydrostatic test; for CVN=15.0, the failure occurred during the simulated fatigue portion of the analysis. All other failures occurred during the simulated hydrostatic test and no additional failures occurred during the fatigue portion. This is true for scenarios 2 through 4 at the same crack size.

Table 8: Analyses Comparisons of Interest

Anomaly / Material	1	2	3	4	5	6	7	8	9	10
1		x	x	x	x				x	
2				x		x				
3										
4										
5										x
6										
7										
8										
9										
10										

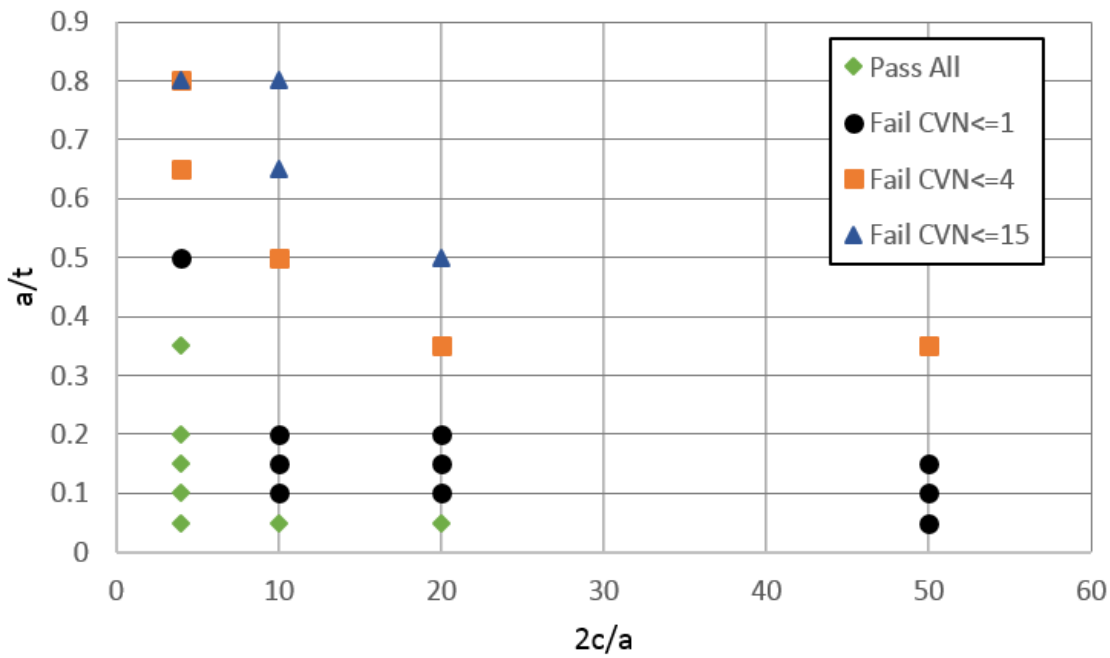

Figure 2: Simulated Hydrostatic Testing Results for X42 ID Cold-Weld using Scenario 1 from Table 7

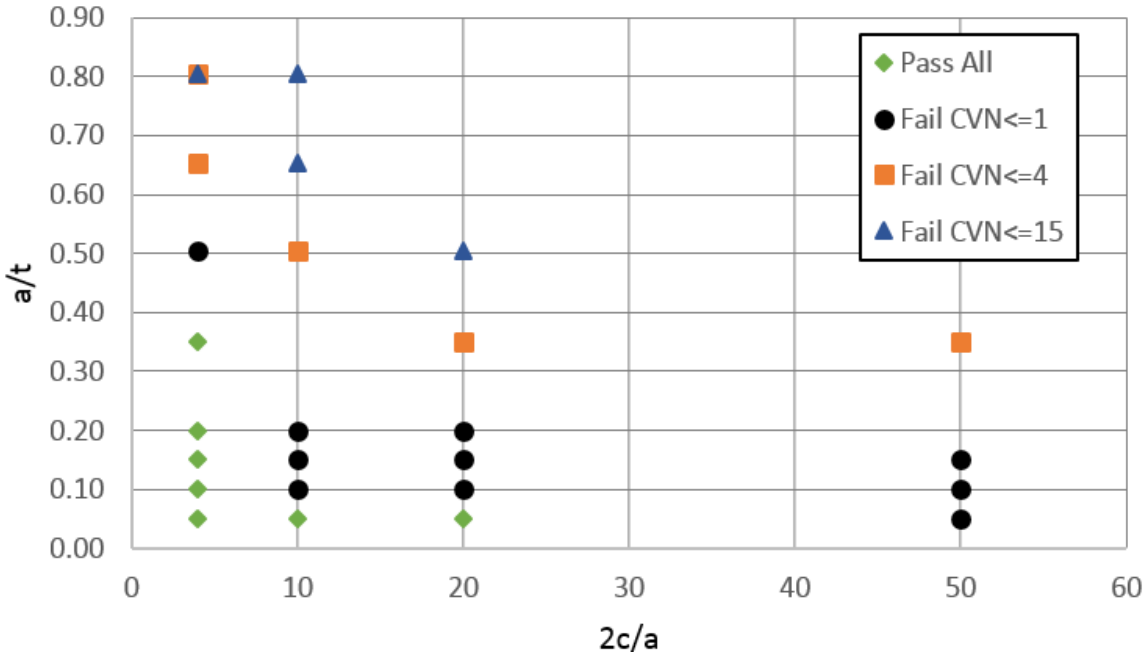

Figure 3: Simulated Hydrostatic Testing Results for X42 ID Cold-Weld using Scenario 2 from Table 7

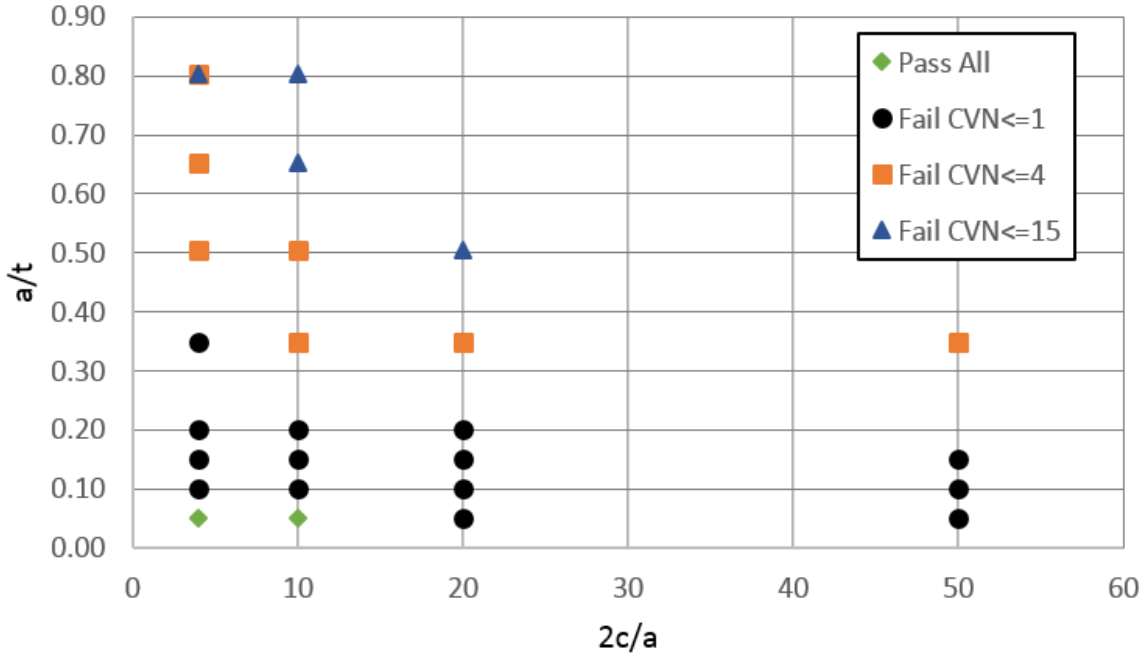

Figure 4: Simulated Hydrostatic Testing Results for X42 ID Cold-Weld using Scenario 3 from Table 7

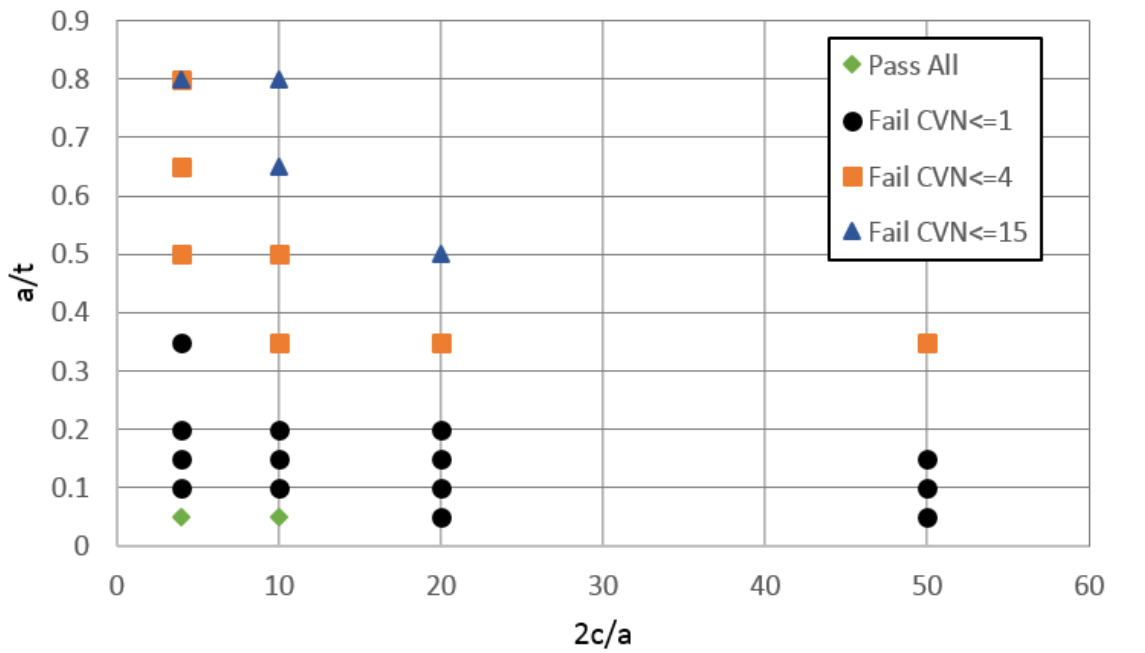

Figure 5: Simulated Hydrostatic Testing Results for X42 ID Cold-Weld using Scenario 4 from Table 7

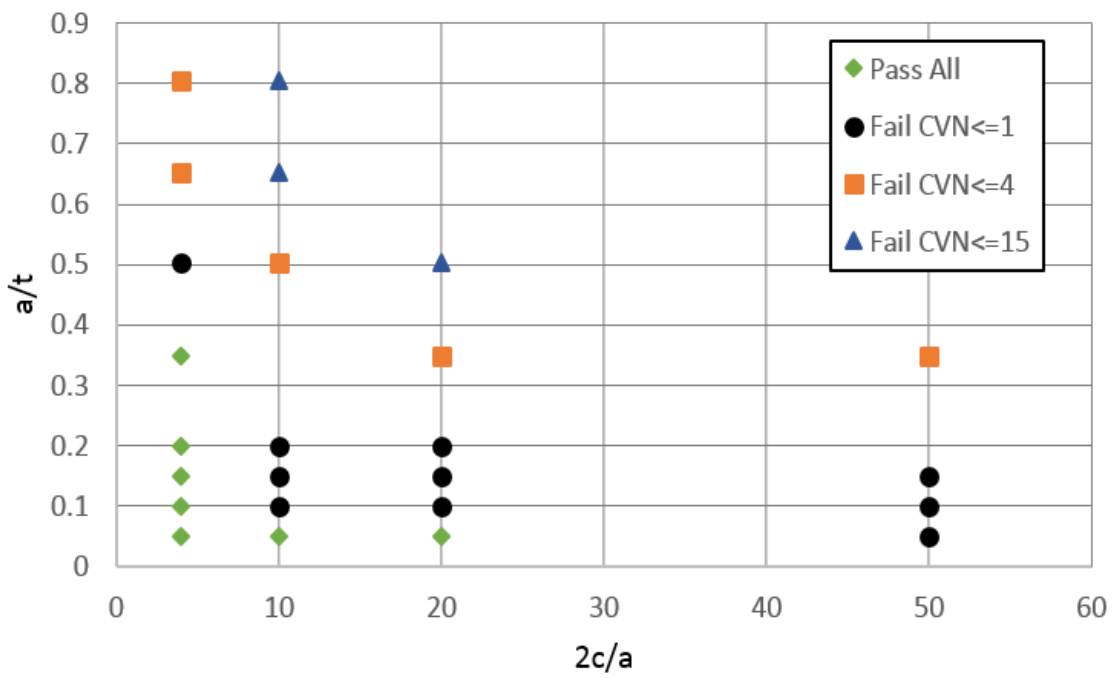

Figure 6: Simulated Hydrostatic Testing Results for X42 ID Cold-Weld using Scenario 5 from Table 7

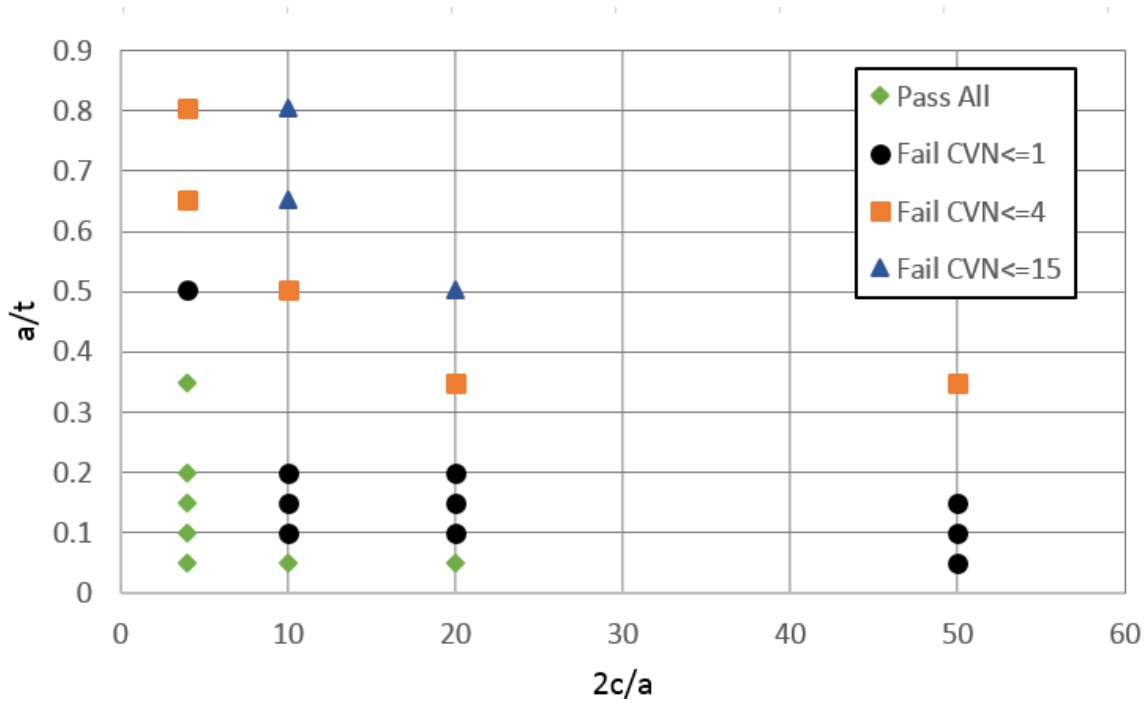

Figure 7: Simulated Hydrostatic Testing Results for X42 ID Cold-Weld using Scenario 6 from Table 7

For scenarios 9 and 10, such that no hydrostatic test was performed prior to fatigue, all simulations survived the fatigue cycling with one exception. For the very aggressive analyses of X42 ID Cold Weld at crack size of a/t = 0.8, 2c/a=4 the initial crack fatigued to failure. The scenarios are discussed in the conclusions section; however, it should be noted that when claims of very aggressive were made for the fatigue profiles in Table 6 and 7 [11], these claims were relative to the models in that reference. As far as can be assessed from the reference, there was no accounting for a threshold stress intensity, no use of a model to account for R-ratio effects, and no model to account for crack tip plasticity due to variation in fatigue loading. Thus, because the models in PipeAssess PI™ account for all of these variations, the very aggressive fatigue loading shows little difference when compared to the "light" fatigue analysis.

Table 9: Summary Comparisons for X42 using a Cold-Weld Anomaly

Scenario Comparison	Figure Comparison	Discussion
1 to 2	2 and 3	Going from Scenario 1 to Scenario 2 provides a comparison of the spike hold times of 10 minutes and 30 minutes respectively. In these simulations, the results are the same. Thus, there is no clear benefit from a simulation perspective of 10 minutes versus 30 minutes. Practical implications will be discussed in the Conclusions section.
1 to 3	2 and 4	Going from Scenario 1 to Scenario 3 provides a comparison of the spike pressures at 100% SMYS and 110% SMYS respectively. The results show as expected with smaller crack sizes failing at higher toughness values for the higher spike pressure. In addition, for those cracks that passed the hydrotest, only the very deep, short crack propagated to fatigue failure, all others did not fail the very-aggressive fatigue loading
1 to 4	2 and 5	Going from Scenario 1 to Scenario 4 provides a comparison of the least aggressive simulated hydrostatic test to the most aggressive simulated hydrostatic test for the given material-anomaly system. The results show as expected with smaller crack sizes failing at higher toughness values for the high spike pressure / longer hold. In addition, for those cracks that passed the hydrotest, only the very deep, short crack propagated to fatigue failure, all others did not fail the very-aggressive fatigue loading (Similar to comparing scenario 1 to 3)
1 to 5	2 and 6	Going from Scenario 1 to Scenario 5 provides a comparison of the least aggressive simulated fatigue test to the most aggressive simulated fatigue test for the given material-anomaly system. The results show as expected with the single fatigue failure in scenario 1, there are no fatigue failures in scenario 5.
2 to 4	3 and 5	As expected, this comparison provides similar results as a comparison of Scenario 1 to Scenario 3.
2 to 6	3 and 7	As expected, this comparison provides similar results as a comparison of Scenario 1 to Scenario 5.
1 to 9	N/A	The comparison of Scenario 1 to Scenario 9 was as expected, the very aggressive fatigue spectrum in Reference [11] was not effective for the model using a threshold stress intensity factor coupled with the Walker and Willenborg models. Additional discussion was in the paragraph preceding the table and in the conclusion section.
5 to 10	N/A	The comparison of Scenario 5 to Scenario 10 was as expected, the light fatigue spectrum was not anticipated to produce any failures in the 5-year test window.

Cold Weld Analyses – X80

Considering the results obtained for the Cold Weld X42 data, the fatigue cycles did not appear to influence the outcome. The Cold Weld X80 analyses, and all subsequent analyses, were reduced to those scenarios listed in Table 10. Results for the analyses are shown in Figures 8 through 10.

Table 10: Analyzed Scenarios for Hydrostatic Test Simulation for Cold Weld X80

Scenario	Spike Stress (%SMYS)	Spike Hold (min)	Fatigue
1	100	10	Very Aggressive
2	100	30	Very Aggressive
3	110	10	Very Aggressive

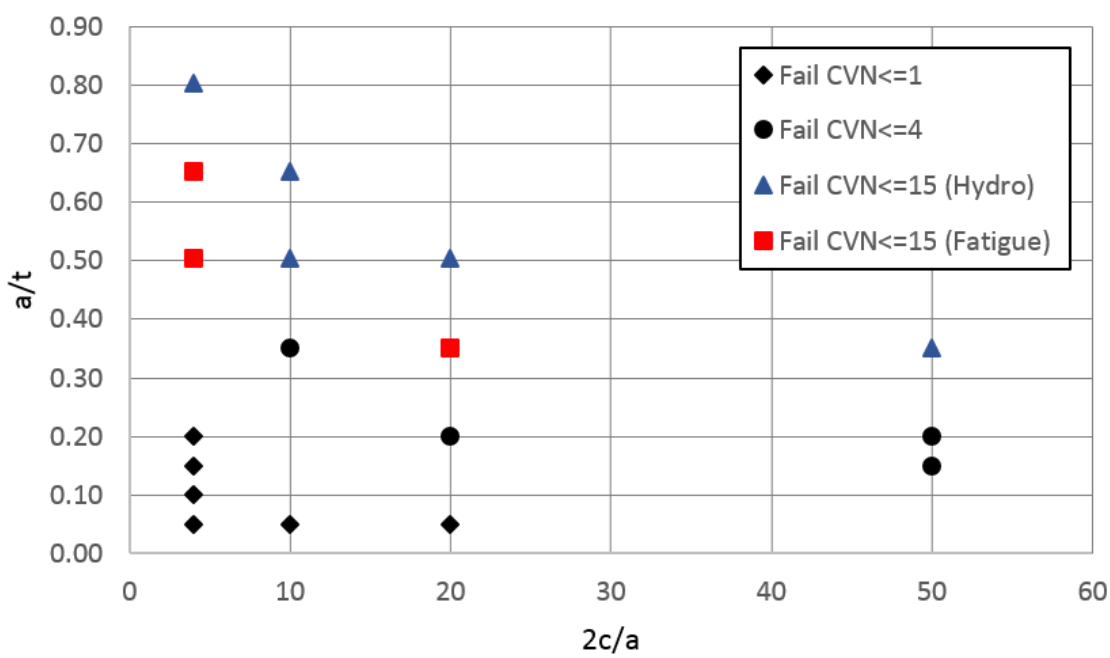

Figure 8: Simulated Results for X80 ID Cold-Weld using Scenario 1 from Table 10

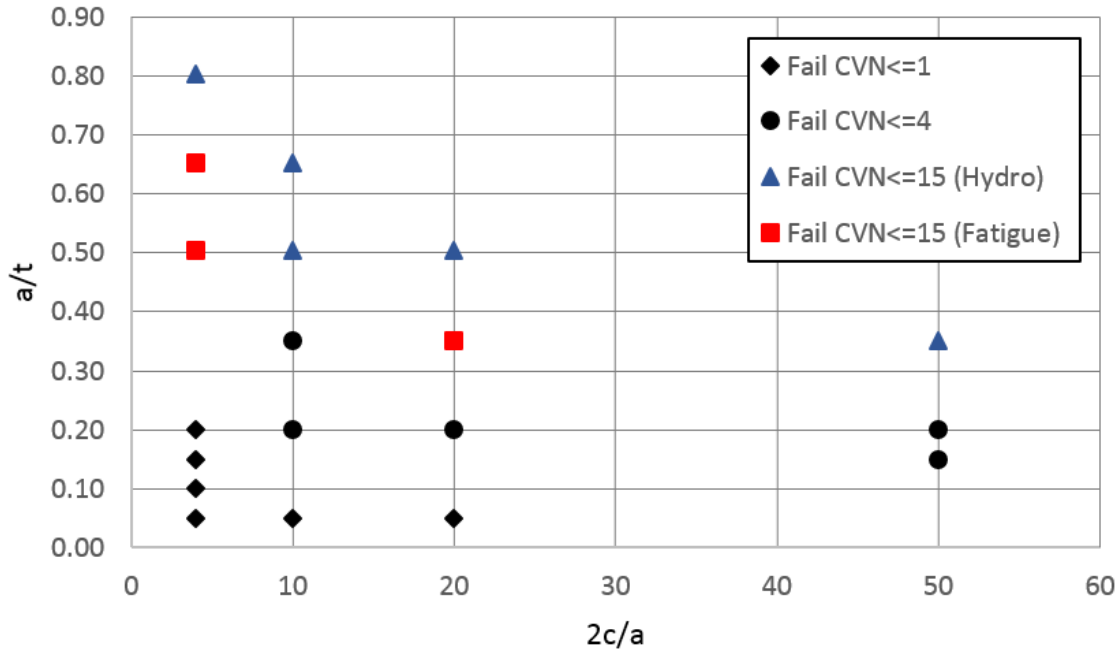

Figure 9: Simulated Results for X80 ID Cold-Weld using Scenario 2 from Table 10

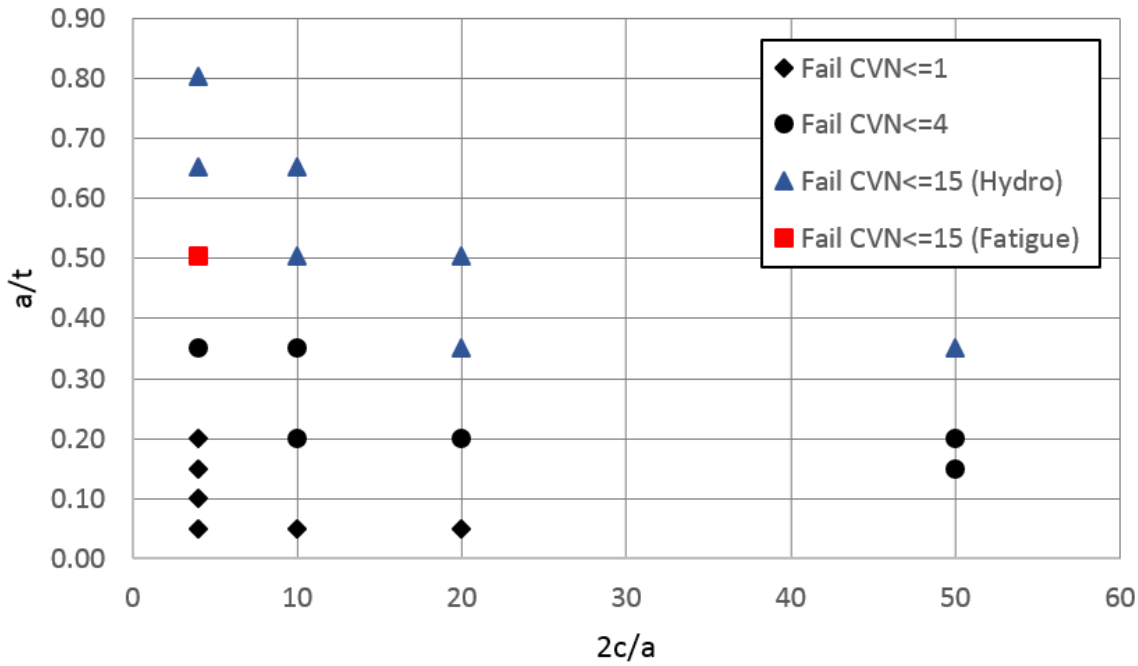

Figure 10: Simulated Results for X80 ID Cold-Weld using Scenario 3 from Table 10

Table 11: Summary Comparisons for X80 using a Cold-Weld Anomaly

Scenario Comparison	Figure Comparison	Discussion
1 to 2	8 and 9	Going from Scenario 1 to Scenario 2 provides a comparison of the spike hold times of 10 minutes and 30 minutes respectively. In these simulations, the results are similar with one point failing (a/t=0.2, 2c/a=10) with the longer spike time that did not fail with the lower pressure. Thus, there is no clear benefit from a simulation perspective of 10 minutes over 30 minutes. Practical implications will be discussed in the Conclusions section.
1 to 3	8 and 10	Going from Scenario 1 to Scenario 3 provides a comparison of the spike pressures at 100% SMYS and 110% SMYS respectively. The results show as expected with smaller crack sizes failing at higher toughness values for the higher spike pressure. In addition, for those cracks that passed the hydrotest, there is a benefit of going to the higher pressure as seen with less fatigue failures for the intermediate crack sizes.

Hook Crack Analyses

For the purposes of this study, hook cracks are embedded with in the pipe wall. A detailed description of the hook crack geometry is given in Reference [16]. Cracks with respect to the geometry are shown in Figure 11. In the analysis software, the only option for the hook crack geometry is infinitely long. This assumption provides a conservative result with respect to failure pressure and precludes the analyses of hydrotest protocols directly. However, a comparison to the failure pressure for infinitely long cold welds with the same crack length leads to the conclusion that for a given hydrotest condition the cold-weld results are conservative with respect to the failure. and a crack of the same through-thickness depth. It should also be noted that based on the work completed in Task 3 [16], the stress intensity factors for embedded flaws are much less than those for surface flaws (i.e. cold weld cracks). Figure 12 provides the failure pressures required for a X80 using an infinitely long surface crack and an infinitely long hook crack. The crack length will be defined as the hypotenuse of the triangle formed by x and y in Figure 11, and the angle beta is defined as the inverse tangent of (x/y).

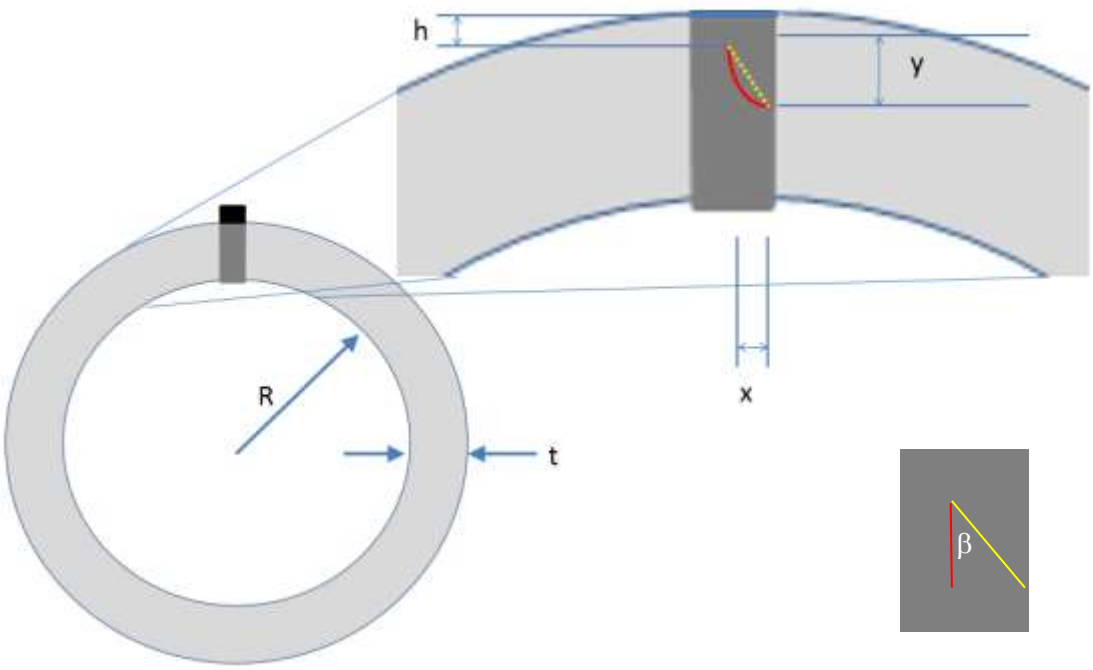

Figure 11: PipeAssess PI™ Hook Crack Geometry Idealization.

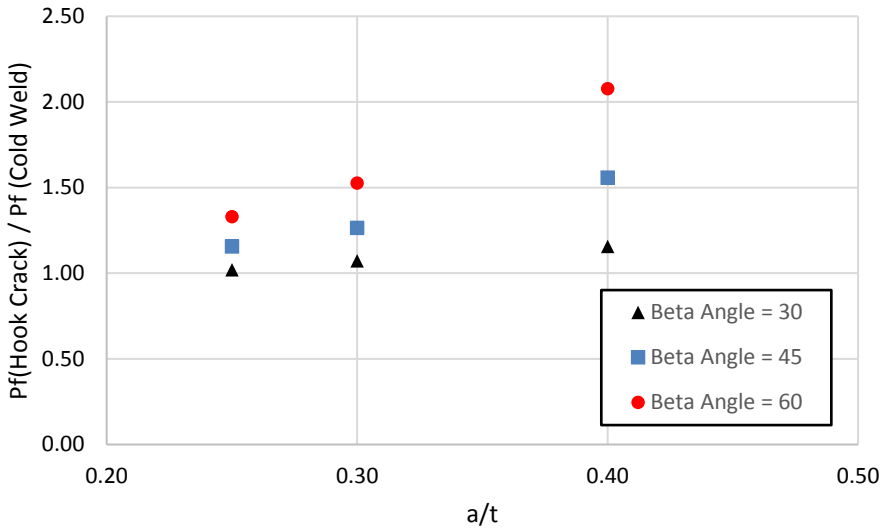

Figure 12: Hook Crack Failure Pressure compared to Cold Weld Failure Pressure

Figure 12 was developed using CVN of 4 ft-lbs with an X80 grade. Based on these results, for a given crack length and CVN value, hook cracks will survive a more robust hydrotest than cold-welds. These results are due to the fact that hook cracks have a lower stress intensity factor for the same size crack.

Selective Seam Weld Analyses

Selective Seam Weld Corrosion (SSWC) cracks have numerous variables to be considered during analyses which may or may not be known to the operator. A detailed description of the hook crack geometry is given in Reference [16]. An example of SSWC Cracks with respect to the geometry are shown in Figure 13. SSWC has multiple configurations which are defined in Reference [16]; however, Figure 13 is representative for the discussion herein. Like the hook crack geometry, the assumption in the software is that the SSWC is infinitely long. This assumption provides a conservative result with respect to failure pressure and precludes the analyses of hydrotest protocols directly.

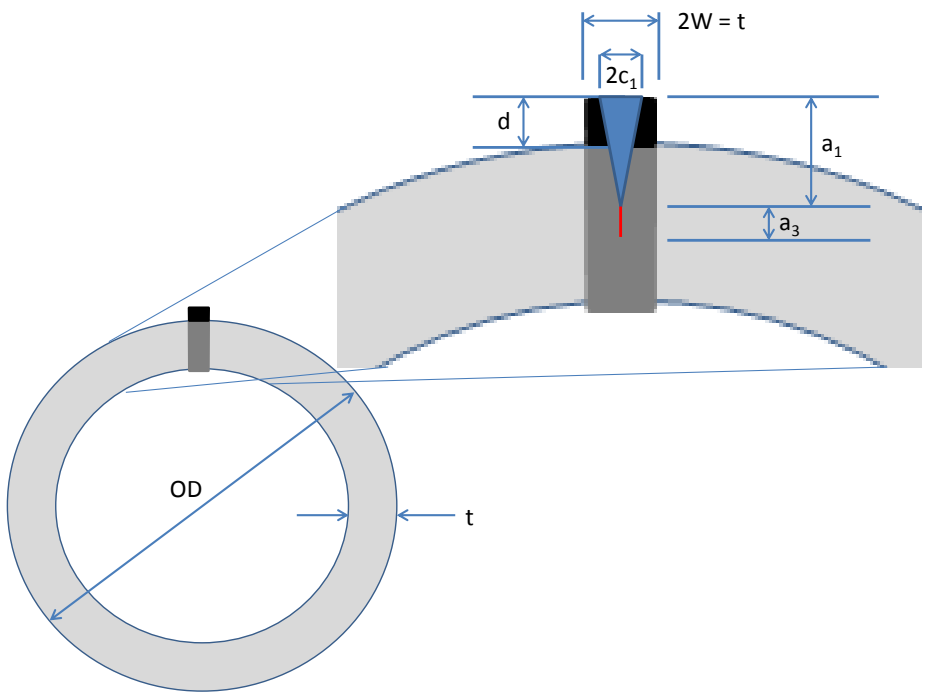

Figure 13: Example - PipeAssess PI™ Selective Seam Weld Corrosion Idealization.

While there is no way to directly compare the SSWC analyses to the cold-weld crack analyses, results would indicate that for a SSWC crack of similar depth (ex: $a_1 + a_3 - d$) when compared to the results of a cold weld crack, the SSWC has a lower failure pressure at a given CVN. This is due to the higher stress-intensity factor (SIF) for a SSWC compared to the cold weld cracks. This high SIF can be rationalized for two reasons, one the local thinning of the pipe wall and two, the lower restraint due to the shape of the selective corrosion ($2C_1$) as show in Reference [16]. Thus, the conclusion is that for a given hydrotest protocol, SSWC cracks (of the same depth) will fail prior to cold weld cracks (for a given toughness).

Conclusions and Recommendation

Based on the results of this study and the information in Reference [3] , the following conclusions are established from the study conducted:

- Large cracks were judged to be invalid a-priori due to their inability to survive at 72% SMYS. This assumption affects the fatigue analyses due to the fact the analyses is only focused on crack sizes that would not failure during operations, rather than hypothetical cracks that would grow in fatigue, but would not survive the 72% SMYS pressure.

- Spike Pressure of 100% to 110% SMYS is sufficient to fail flaw sizes commensurate with the pipe grade (SMYS) and expected ERW toughness (Charpy)

    - Small to intermediate flaws (i.e. below the ILI detection limit are predicted to fail when Charpy toughness are less than 4 ft-lb (i.e. low toughness bondlines)

    - Large flaws are predicted to fail even when Charpy toughness values as high as 15 ft-lbs. For example, a 35% through-wall flaw that is 2-inches long would fail the standard hydrostatic test as shown in Figure 10 (a/t=0.25, 2C/a = 20)

- There is no benefit of reduced hydrotest failures, via the simulations, by reducing the simulated spike time from 30 minutes to 10 minutes.

- Crack geometry plays an important role in consideration of hydrostatic testing. While a given size hook-crack may be benign to pressures up to 72% SMYS, once the crack becomes surface breaking, the driving force for a given pressure could be an order of magnitude greater.

- Definition of “very aggressive” fatigue profile is ambiguous in the context of these analyses. While the fatigue spectrum is well defined in Reference [11], the use of this spectrum coupled with the threshold stress intensity model [17], the effective R-ratio model [13], and the crack tip overload model [14] seems to reduce the aggressiveness of the spectrums.

- Fatigue cycles were applied post-hydrotest for 5 years.

    - Model predictions indicate that a Spike Pressure of 100% to 110% SMYS creates a sufficient plastic zone size to retard fatigue growth for most crack-like defects.

  - With the very-aggressive hypothetical fatigue spectrum, crack growth occurred, and fatigue failures were predicted for only very short, deep cracks within the 5 years analyzed.

- X80 tends to be more sensitive to the simulated hydrostatic test analyses. With low Charpy energy, the hydrostatic test considerations of 100% SMYS and 110% SMYS provide failures with lower crack dimensions as compared to the X42. This is due to the absolute stress driving the failure rather than the relative stress to SMYS.

- X80 tends to be more sensitive to the simulated fatigue analyses. As compared to X42, for a given profile (as % SMYS), the X80 tends to have accelerated crack growth due to a larger absolute stress intensity range.

- For a hook crack of the same depth as a cold weld crack with assumed equal Charpy toughness values, the hook crack has a lower stress intensity factor, thus is expected to survive a more aggressive hydrotest than a similar cold weld crack.

- For a SSWC crack of the same depth as a cold weld crack, with assumed equal Charpy toughness values, the SSWC crack has a higher stress intensity factor, thus is prone to failure at a less aggressive hydrotest than a similar cold weld crack.

While the conclusions provided are beneficial, additional considerations should be undertaken and understood when completing hydrostatic tests. This study was conducted assuming a MAOP of 72% SMYS, but for lines being operated at an MAOP much less than 72% SMYS, additional factors should be considered beyond the guidance provided here (i.e. valve and tap locations where pressure ratings are lowered).

Other considerations should include

- Practical considerations should be undertaken to understand the realistic time to conduct a spike test in field applications.

- To ensure adequate leak detection, leak checks should be conducted (i.e. after spike test) at 90% of SMYS.

- Variation in terrain (i.e. elevation) should be considered when designing the hydrotest, as should the length of the test section. Changes in elevation may require more frequent and shorter test sections.

- Active corrosion growth, i.e. stress corrosion cracking or selective seam-weld corrosion, was not considered as part of this analysis for the post-hydrotest investigation.

While the research outlined in this report was intended to be a comprehensive study to understand longitudinal ERW seam failure, consideration of future work on the hydrotest protocols beyond the work completed as part of Phase II, Task 1 may be warranted. The work conducted herein relied on data that had been developed for specific material Grades. While most grades have been studied, and time dependent Ramberg-Osgood parameters have been identified, there are still gaps in the data. Two examples of these gaps are data for Grade B and Grade X60 pipe.

Works Cited

[1] B. N. Leis, F. W. Brust and P. M. Scott, "NG-18 Report No. 193: Development and Validation of a Ductile Flaw Growth Analysis for Gas Transmission Line Pipe," American Gas Association, 1991.

[2] B. N. Leis and F. W. Brust, "NG-18 Report No. 194: Hydrotest Strategies for Gas Transmission Pipelines Based on Ductile-Flaw-Growth Considerations," American Gas Association, 1992.

[3] R. J. Olson, B. A. Young and B. Leis, "Findings from an Investigation of Hydrotest Protocols," in *ASME IPC 2016*, Calgary, 2016.

[4] T. Anderson and G. Throwald, "A Fintie Element Procedure to Model the Effect of Hydrostatic Testing on Subsequent Fatigue Crack Growth," in *ASME IPC 2016*, Calgary, 2016.

[5] N. Al-Otaibi, H. Al-Muslim, W. Harper, T. Bubenik and W. A. Al-Usaimi, "Assessing the Benefits of Hydrotests for Pipelines with SCC History Post-Detection ILI Runs," in *ASME IPC 2016*, Calgary, 2016.

[6] M. Hilger, B. Mittelstadt and M. V. P. Piazza, "Pipeline Oporator Perspective in Use of Hydrostatic Testing as an Integrity Management Tool," in *ASME IPC 2016*, Calgary, 2016.

[7] D. Warman, N. Grusdowich, H. Kleeman, S. Boardman and U. Duruike, "De Facto Hydrostatic Test Pressures - A Study in Double Stroking," in *ASME IPC 2016*, Calgary, 2016.

[8] J. Rau and M. Kirkwood, "Hydrotesting and In-Line Inspection; Now and in the Future," in *ASME IPC 2016*, Calgary, 2016.

[9] S. Keane, M. Rosenfeld and L. Heise, "Hydrostatic Pressure Testing as Part of an Integrity Magagement Program: A Case Study," in *ASME IPC 2016*, Calgary, 2016.

[10] Hryciuk, P.M., Carzoglio, E., Minellono, J., et al., "The Use of Hydrotesting and EMAT Inline Inspection Technology for the Integrity Managment of Stress Corrosion Cracking (SCC) in Gas Pipelines," in *ASME IPC 2016*, Calgary, 2016.

[11] Micheal Baker Jr., Inc., "TTO Number 5, Intergrity Managment Program Delivery Order DTRS56-020D070036, Low Frequency ERW and Lap Welded Longitudinal Seam Evaluation; Final Report - Rev 3.," Department of Transportation, Research and Special Programs Administration, Office of Pipeline safety, 2014.

[12] B. N. Leis and F. W. Brust, "Hydrotest Strategies for Gas Transmission Pipelines Based on Ductile Flaw Growth Considerations Pipelines Based on Ductile Flaw Growth Considerations," Pipeline Research Council International, PRCI/AGA Catalog No. L51665, 1992.

[13] D. Lombardo and J. Paul, "Aircraft Structures Technical Memorandom 492," 1988. [Online]. Available: www.dtic.mil/cgi-bin/GetTRDoc?AD=ADA199552.

[14] J. Willenborg, R. Engle and H. and Wood, "A Crack Growth Retardation Model Ising an Effective Stress Approach," Air Force Flight Dynamics Laboratory, Wright Patterson Air Force Base, Ohio, 1971.

[15] *Proprietary Data Held at Battelle*, 2015.

[16] B. Young, J. O'Brian and R. Olson, "Defect Characterization: Types, Sizes, Shapes, and Idealizations," Battelle Memorial Institute, Columbus, 2017.

[17] B. Young, J. O'Brian and R. Olson, "Validation of Fatigue Models for ERW Seam Weld Cracking", in ASME PVP-2017, Waikola, 2017